In Vitro Cell. Dev. Biol.—Animal 41:207–216, July–August 2005

1071-2690/05 $18.00+0.00

EFFECT OF THE MODULATION OF THE MEMBRANE LIPID COMPOSITION ON THE LOCALIZATION AND FUNCTION OF P-GLYCOPROTEIN IN MDR1-MDCK CELLS

SARAH W. KAMAU,[1] STEFANIE D. KRÄMER, MAJA GÜNTHERT, AND HEIDI WUNDERLI-ALLENSPACH

Institute of Veterinary Biochemistry and Molecular Biology, University of Zurich, Winterthurerstrasse 190, CH-8057 Zurich, Switzerland (S. W. K.), and Institute of Pharmaceutical Sciences, ETH Federal Institute of Technology, Wolfgang-Pauli-Strasse 10, CH-8093 Zurich, Switzerland (S. D. K., M. G., H. W.-A.)

(Received 18 February 2005; accepted 13 April 2005)

SUMMARY

Multidrug resistance (MDR) is a major obstacle in cancer therapy. It results from different mechanisms; among them is P-glycoprotein (P-gp)–mediated drug efflux out of cells. The mechanism of action remains elusive. The membrane lipid surrounding of P-gp, especially cholesterol, has been postulated to play an important role. To determine the effect of cholesterol depletion on P-gp, Madin Darby canine kidney (MDCK) cells, transfected with the *mdr1* gene (MDR1-MDCK cells), were treated with methyl-β-cyclodextrin (MβCD). The localization and function of P-gp were analyzed using confocal laser scanning microscopy. Treatment with 100 m*M* MβCD did not affect viability but altered the structural appearance of the cells and abolished efflux of rhodamine 123, a P-gp substrate. The MβCD treatment released P-gp from intact cells into the supernatant and reduced the amount of P-gp in total membrane preparations. The P-gp was shifted from the raft fractions (1% Triton X-100, 4° C) to higher density fractions in MβCD-treated cells. The amount of cholesterol was significantly decreased in the raft fractions. Treatment of cells with 1-phenyl-2-decanoylamino-3-morpholino-1-propanol, a glucosylceramide synthase inhibitor, also led to a shift of P-gp to higher density fractions. These results show that removal of cholesterol modulates the membrane lipid composition, changes the localization of P-gp, and results in loss of P-gp function.

Key words: P-glycoprotein; cholesterol; glycosphingolipids; rafts.

INTRODUCTION

The expression of multidrug resistance proteins at the blood–brain barrier (BBB), in tumor tissue, and in T cells prevents many pharmacologically potent central nervous system, antitumor, or anti-human immunodeficiency virus drugs from reaching their target. The human multidrug resistance (MDR1), P-glycoprotein (P-gp), belongs to the adenosine triphosphate (ATP)-binding cassette superfamily of membrane transporters. The P-gp transports compounds in an unmodified state and is therefore of particular interest for drug uptake, distribution, and elimination. It has primarily been described as a drug efflux pump, which mediates multidrug resistance. The extent to which P-gp and other multidrug resistance proteins directly pump compounds across the plasma membrane of cells or translocate them between the two membrane leaflets is not clear, nor is to what extent their drug transport capability is based on lipid sorting, thus influencing the physicochemical characteristics of the plasma membrane (Sharom, 1997; Roepe, 1998; Eytan and Kuchel, 1999). There is strong evidence that the lipid composition of biological membranes and the function of proteins such as P-gp are closely related (Modok et al., 2004; Norris-Cervetto et al., 2004; Troost et al., 2004).

In Madin Darby canine kidney (MDCK) cells, stably transfected with the *mdr1* gene (MDR1-MDCK cells), P-gp is highly expressed and homogenously distributed on the cell layer already a few days after seeding. This is in contrast to Caco-2 cell cultures that express P-gp after 2–3 wk in lower amounts and limited to patches of the cell layer (Braun et al., 2000; Hammerle et al., 2000; Tang et al., 2002). The P-gp is primarily localized in the apical plasma membrane (Simons and Ikonen, 1997; Hammerle et al., 2000; Luker et al., 2000), which is enriched in cholesterol, glycosphingolipids (GSLs), and sphingomyelin (SM) (Simons and van Meer, 1988; Hooper, 1999). The MDR1-MDCK cells thus represent an ideal system to study the influence of the modulation of lipids on the localization and function of the P-gp.

The P-gp is predominantly localized in low-density caveolae-enriched domains (rafts) (Lavie et al., 1998; Demeule et al., 2000; Luker et al., 2000). To better understand the role of the lipid environment on proteins, different methods have been developed to isolate specific membrane domains (Hooper, 1999; Pike, 2003a, 2003b). Detergent-resistant rafts, prepared in cold buffer containing 1% Triton X-100 (Brown and Rose, 1992), are enriched in cholesterol and GSLs (Pike, 2003a); hence, their role on the localization and function of P-gp is of interest.

To determine the effect of modulation of cholesterol and GSLs in MDR1-MDCK cells, cholesterol was depleted with methyl-β-cyclodextrin (MβCD) (Ilangumaran and Hoessli, 1998), and the synthesis of GSLs was inhibited with 1-phenyl-2-decanoylamino-3-morpholino-1-propanolol (PDMP) (Lavie et al., 1997, 1999; Lucci et al.,

[1] To whom correspondence should be addressed at E-mail: kamau@vetbio.unizh.ch

1999; Sietsma et al., 2000; Plo et al., 2002). The localization of P-gp and the efflux of rhodamine 123 (rho123), a P-gp substrate, in MβCD-treated cells were studied using confocal laser scanning microscopy (CLSM). The release of P-gp from viable cells and from total membrane preparations after MβCD treatment was detected by immunoblotting. Lipid rafts were prepared in cold buffer containing 1% Triton X-100, from MβCD- or PDMP-treated cells and untreated cells, and P-gp and lipid distributions in rafts and nonraft fractions were analyzed by immunoblotting and thin layer chromatography (TLC), respectively.

Materials and Methods

Cell culture and treatment with MβCD and PDMP. The MDCK cells transfected with the *mdr1* gene (MDR1-MDCK) were a gift from Ira Pastan. They were propagated in Dulbecco modified Eagle medium with Glutamax-I (Invitrogen AG, Basel, Switzerland), as described previously (Pastan et al., 1988; Hammerle et al., 2000). The CLSM studies were performed on cell cultures grown on cell culture inserts, whereas the other experiments were performed on cell cultures grown in plastic culture flasks (Hammerle et al., 2000). In all experiments, the passage number was below 50 and unless otherwise stated, cell cultures were used 11 d after seeding, which corresponded to the stationary growth phase (Braun et al., 2000; Hammerle et al., 2000). In the subsequent experiments, all solutions contained protease inhibitors, and the experiments were performed at least three times.

Stock solutions of 200 and 500 m*M* MβCD (Wacker Chemie AG, Burghausen, Germany) were prepared in distilled water. Cells were incubated for 1 h in serum-free medium before they were treated with 20, 30, or 100 m*M* MβCD for 30 min, 1 h, and 2 h, respectively, at 37° C. Untreated control cells were prepared similarly to the MβCD-treated cells. The supernatants above the control and MβCD-treated cells in the culture flasks were collected for further processing. The culture flasks were rinsed thrice with Earle's balanced salt solution (EBSS) (Invitrogen) before the cells were harvested by scraping and subsequently washed thrice with phosphate-buffered saline (PBS; 10 m*M* Na_2HPO_4–KH_2PO_4, 130 m*M* NaCl, pH 7.4) before being processed, as indicated below.

To determine the effect of PDMP, cell cultures were grown for 9 d before 30 μ*M* PDMP (Sigma–Aldrich, Buchs, Switzerland) was added in fresh medium (di Bartolomeo and Spinedi, 2001). The cells were incubated for 48 h at 37° C, rinsed thrice with EBSS, and harvested by scraping before being used for raft preparation as described below.

Immunofluorescent labeling. The cells were prepared for CLSM, as described previously (Pastan et al., 1988; Rothen-Rutishauser et al., 1998; Hammerle et al., 2000). The following antibodies, diluted in PBS containing 3% (w/v) bovine serum albumin and 0.1% (w/v) saponin, were used for labeling: mouse monoclonal 4E3 anti–P-gp (Dako Diagnostics AG, Copenhagen, Denmark) 1:10, mouse monoclonal antioccludin (Zymed Laboratories Inc., San Francisco, CA) 1:100, and rabbit anticaveolin (BD Transduction Laboratories, San Jose, CA) 1:100. Anti-rabbit cyanine 3 and anti-mouse cyanine 3 (Sigma) 1:50, were used as secondary antibodies. F-actin was stained with Alexa Fluor 660 phalloidin 1:50 and nuclei with 1 μg/ml 4′,6-diamidino-2-phenylindole (DAPI) (Molecular Probes, Leiden, The Netherlands). Preparations were studied with a Zeiss LSM 410 inverted microscope, and for image reconstruction, the IMARIS software (Bitplane, Zurich, Switzerland) was used (Hammerle et al., 2000).

The rho123 efflux assay. The efflux assay was performed, as described previously (Fontaine et al., 1996; Hammerle et al., 2000). The efflux of rho123 (Sigma) was observed in the CLSM by z-scans of the cell layers and of the adjacent apical extracellular space. For a better orientation, the nuclei were stained using Hoechst 33342 (Molecular Probes). For P-gp inhibition studies, 0.1 m*M* verapamil hydrochloride (Sigma) was added 5 min before the addition of rho123 and Hoechst 33342 and to all solutions throughout the assay.

Viability tests. The viability of MβCD-treated and untreated cells was determined using the Live/Dead viability/cytotoxicity Kit that contained the two fluorescent probes, calcein AM and ethidium homodimer–1 (Molecular Probes). Calcein AM is cleaved by cytosolic esterases to its green fluorescent metabolite calcein in live cells, whereas ethidium homodimer–1 permeates dead cells and stains their nuclei red (Neethling et al., 1999; Wagner et al., 1999). To some of the control cells, 0.1 m*M* verapamil was added before staining with Live/Dead Kit to inhibit the P-gp efflux function because calcein AM is a P-gp substrate (Loor et al., 2002; Kohler and Stein, 2003). An additional control, of nonviable MDR1-MDCK cells, rinsed thrice with hot EBSS, was also included in the assay. The viability of MβCD-treated cells was additionally tested in 96-well plates using the (3-(4,5-dimethylthiazol-2-yl)-2,5-diphenyl tetrazolium bromide (MTT) assay (Mosmann, 1983; van de Loosdrecht et al., 1994).

Preparation of total membranes and treatment with MβCD. Total membrane fractions were prepared, as described previously (Ilangumaran and Hoessli, 1998). In brief, 2.5×10^8 cells were resuspended in 5 ml of hypotonic buffer (10 m*M* Tris–HCl, 10 m*M* KCl, 5 m*M* $MgCl_2$, 1 m*M* ethylene glycol-bis(aminoethylether)-tetraacetic acid, pH 7.4) and homogenized using a Dounce homogenizer (50 strokes, 1000/min). After centrifugation at 2000 × *g* for 10 min at 4° C, the supernatant was layered over 5 ml of 40% (w/v) sucrose in Tris-NaCl-EDTA buffer (TNE) buffer (25 m*M* Tris–HCl, 150 m*M* NaCl, 5 m*M* ethylenediaminetetraacetic acid [EDTA], pH 7.4) and centrifuged at 100,000 × *g* for 1 h at 4° C. The light scattering band containing the total membranes, above the sucrose cushion was collected and divided into four fractions, which were treated with MβCD, as stated above, with intermittent shaking. Subsequently, the sample volumes were adjusted to 5 ml with the TNE buffer and layered over 5 ml of 40% (w/v) sucrose, and the procedure was repeated as described above. After centrifugation, the volume of the resulting membrane fractions were adjusted to 3 ml with TNE buffer, and samples centrifuged at 250,000 × *g* for 3.5 h at 4° C. The pellets were collected and dissolved in 100 μl sample buffer (Laemmli, 1970).

Differential centrifugation of cell supernatant. The supernatants from 2.5×10^6 MβCD-treated and untreated cells were collected and centrifuged at 2000 × *g* for 10 min at 4° C. The cell-free supernatants were further centrifuged at 10,000 × *g* for 15 min at 4° C in a S4180 rotor (Beckman Instruments). The pellets were collected and dissolved in 100 μl sample buffer for sodium dodecyl sulfate–polyacrylamide gel electrophoresis (SDS-PAGE) and immunoblotting or in 300 μl chloroform–methanol (2:1, v/v), for lipid analysis.

Preparation of rafts. Rafts were prepared as described previously (Brown and Rose, 1992); in brief, 2.5×10^8 MβCD-treated and untreated cells were lysed for 20 min on ice in 2 ml TNE buffer containing 1% (v/v) Triton X-100 (Laemmli, 1970; Brown and Rose, 1992). After homogenization, the homogenate was mixed with an equal volume of 80% (w/v) sucrose solution in TNE buffer and overlaid with a discontinuous sucrose gradient (2 ml each of 30, 20, 10%, and 1.5 ml of 5% [w/v] sucrose, all in TNE buffer without Triton X-100). After centrifugation at 200,000 × *g* for 19 h at 4° C, in a SW41Ti rotor (Beckman Instruments, Fullerton, CA), 1 ml fractions were collected from the top of the gradient (fractions 1–12) without including the pellet at the bottom. Raft fractions 4–7 had higher optical densities (620 nm) than the rest of the fractions (Hooper, 1999) and densities of 1.06–1.13 g/cm³, calculated from their respective refractive indices (refractometer, Bellingham and Stanley Inc., Tunbridge Wells, U.K.). The size intensity distribution and polydispersity factor, determined with a Zetasizer 3 (Malvern Instruments, Worcestershire, UK), gave the "average mean diameter" of 265.8 ± 5.8 nm, with a mean polydispersity factor of 0.45 ± 0.03. The distribution of protein along the gradient was characteristically skewed, with most protein being concentrated within fractions 7–12 (density range 1.13–1.20 g/cm³). Each fraction was sedimented similarly to the membrane fractions and the pellets dissolved in 100 μl sample buffer for SDS-PAGE and immunoblotting.

The SDS-PAGE and immunoblots. Dissolved samples were analyzed immediately or stored at −70° C. The protein concentrations were determined with the Bio-Rad D_C protein assay (Bradford, 1976). Samples were denatured by heating for 5 min at 95° C, before being loaded onto a 7.5% (w/v) gel for P-gp detection (4 μg protein/slot) or onto a 15% (w/v) gel for caveolin detection (2 μg protein/slot). After SDS-PAGE and Western blotting (Hammerle et al., 2000), the antibody labeling was performed with the monoclonal mouse anti-human P-gp antibody C219 (Dako) or rabbit antiactin (Sigma) (1:500) or with rabbit anticaveolin antibody (1:5000). The nitrocellulose membranes were subsequently incubated with the anti-mouse (1:30,000) and anti-rabbit (1:50,000) secondary antibodies conjugated with alkaline phosphatase (Pierce Biotechnology, Rockford, IL). They were analyzed with an enhanced chemiluminescence immunoblotting detection system (BioRad Laboratories Inc., Hercules, CA).

Lipid analysis. For lipid analysis, 4.1×10^7 cells were washed and harvested by scraping, and lipids were extracted from the cell pellet using 1 ml of chloroform–methanol (2:1, v/v). Lipids were identified and quantified, as

described previously (Brown and Rose, 1992; Kramer et al., 2002). In brief, 25 μl of the lipid extracts were applied onto TLC silicagel 60 aluminum sheets (Merck, Darmstadt, Germany) together with a series of different volumes (1–25 μl) of the reference stock solution (Shand and Noble, 1980; Kramer et al., 2002). Polar lipids were developed with chloroform–methanol–acetic acid–water (60:50:1:4, v/v), neutral lipids in heptane–diethylether–acetic acid (60:40:2, v/v), and GSLs in chloroform–methanol–water (65:25:4, v/v). The dried TLC sheets were sprayed with an aqueous solution of 3% (w/v) cupric acetate and 8% (v/v) phosphoric acid (Shand and Noble, 1980). The dried sheets were heated for 15 min at 180° C to char the lipids. The TLC plates were scanned and subsequently analyzed by the computer program Scion Image (Scion Corp., Frederick, MD) using the macro gelplot2. The dark spots were thus converted to density peaks, which were quantified by the area under the curve (AUC). The correlation between the AUCs and the lipid concentrations of the reference spots was determined and used to calculate the concentrations of the extracted lipids (Kramer et al., 2002).

Lipid analysis of the raft and nonraft fractions was performed on fractions separated on a discontinuous sodium bromide (NaBr) gradient instead of a sucrose gradient. The homogenate was mixed with an equal volume of 64% (w/v) sodium bromide stock solution in PBS. The sample was overlaid with 2 ml of 1.73 *M* NaBr, 2 ml of 0.87 *M* NaBr (both in 0.2 *M* NaCl and 0.34 m*M* EDTA, pH 7.78), and 2 ml PBS. After centrifugation, 1-ml fractions were transferred into cellulose membrane dialysis tubes (Sigma) and dialyzed against distilled water for 8 h at room temperature. The fractions were then lyophilized overnight at −20° C in 20-ml, thick-walled glass bottles. The residue was transferred into 1.5-ml Eppendorf tubes containing 1 ml of chloroform–methanol (2:1, v/v), and the tubes were placed on a shaker overnight at 4° C. The supernatant containing the lipids was collected after 5 min centrifugation in a microfuge, and the lipids were analyzed, as indicated above.

The amount of cellular, nonesterified cholesterol in 100 m*M* MβCD-treated and untreated cells was additionally determined using the Amplex® Red Cholesterol Assay Kit (Zhou et al., 1997).

Results

Localization of P-gp, caveolin, and occludin in MβCD-treated cells. The CLSM showed no significant difference between control cells (Fig. 1*A–C*) and cells treated with 30 m*M* of MβCD for 1 h (Fig. 1*D–F*). In both cases, most of the P-gp was located in the apical plasma membrane of the topmost layer of cells. However, treatment with 100 m*M* MβCD for 2 h resulted in an apparent decrease of P-gp at the apical plasma membrane. The appearance of the immunolabeling was changed to a punctuate pattern, and the cells started to round up (Fig. 1*G* and *H*).

The localization and distribution of the raft protein caveolin and the tight-junction protein occludin were also studied using CLSM. There was no significant difference between the distribution of caveolin in control (Fig. 2*A–C*) and in 100 m*M* MβCD-treated cells (Fig. 2*D–F*). In cells treated with 100 m*M* MβCD (Fig. 2*J–L*), occludin was still found at the cell borders; however, the tight junctions appeared loosened and swollen when compared with the control cells (Fig. 2*G–I*). Some intracellular labeling of occludin was also observed.

The P-gp efflux function and viability of MβCD-treated cells. Confocal microscopy showed that rho123 was effluxed to the extracellular space in control cells and in cells treated with 20 m*M* MβCD for 30 min (Fig. 3*A* and *C*). Treatment with 30 m*M* MβCD for 1 h also resulted in efflux; however, some of the rho123 was retained within the cells (Fig. 3*E*). The efflux was completely inhibited by treatment with 100 m*M* MβCD for 2 h (Fig. 3*G*). A similar effect was observed in cells treated with verapamil, a known inhibitor of P-gp efflux activity, independent of the MβCD treatment (Fig. 3*B*, *D*, *F*, and *H*).

To exclude the possibility that the loss of efflux activity after treatment with 100 m*M* MβCD, which could be because of a loss of cell viability, the calcein AM–ethidium homodimer viability assay was performed. Cells remained viable after treatment with 30 and 100 m*M* MβCD for 1 and 2 h, respectively, as indicated by the green staining of cells and the lack of red nuclei (Fig. 4*D* and *E*). In contrast, in nonviable cells, no calcein was detected, and ethidium homodimer permeated the cells resulting in red staining of the nuclei (Fig. 4*C*). The green calcein staining of control cells was stronger after verapamil incubation because the efflux of calcein AM by P-gp was inhibited (Fig. 4*A* and *B*) (Kohler and Stein, 2003). The MTT assay results showed that none of the MβCD concentrations used in our study did affect the viability of the cells. The metabolic activity of cells treated with 100 m*M* MβCD remained 109 ± 22% of the control cells.

Effects of MβCD treatment on P-gp and caveolin in total membranes and in supernatants. Treatment of membrane fractions with 100 m*M* MβCD for 2 h resulted in a significant decrease in the amount of P-gp (Fig. 5*A*). In contrast, the amount of caveolin in the total membranes was not affected by MβCD treatment.

Analysis of the supernatants of control and cells treated with 20 m*M* MβCD for 30 min showed that only traces of P-gp were detected in the 10,000 × *g* pellets. In contrast, a substantial amount of P-gp was released after treatment of cells with 50 m*M* MβCD for 30 min and to an even higher extent after treatment with 100 m*M* MβCD for 2 h (Fig. 5*B*). Caveolin and actin were present in all supernatants independent of MβCD treatment (Fig. 5*B* and data not shown).

Distribution of P-gp and caveolin in raft and nonraft fractions prepared from cells treated with either MβCD or PDMP. In control cells, there was an enrichment of P-gp in the raft fractions at a density range of 1.06–1.13 g/cm³ (Fig. 6*A*). A tendency for the distribution of P-gp over a slightly wider density range (1.06–1.15 g/cm³) was detected in cells treated with 20 m*M* of MβCD for 30 min, and treatment of cells with 100 m*M* MβCD for 2 h resulted in a significant shift of P-gp from the raft fractions to higher density fractions (1.18–1.20 g/cm³). Only a small amount of P-gp remained in the raft fractions of cells treated with 100 m*M* MβCD. A similar shift was also observed after treatment of cells with PDMP for 48 h. The distribution of caveolin was not significantly affected by these treatments (Fig. 6*B*).

Lipid composition of cell lysates and raft and nonraft fractions of cells treated with either MβCD or PDMP. Glycerophospholipids (phosphatidylserine, PS; phosphatidylethanolamine, PE; phosphatidylcholine; and phosphatidylinositol) represented 55% (mol/mol) of total analyzed lipids in cell lysates of control cells. Cholesterol was the most abundant lipid accounting for 30%, whereas GSLs represented 9% of the total lipids (Fig. 7*A*). Treatment of cells with 100 m*M* MβCD reduced the amount of cholesterol in the cell lysates to 21.4 ± 4.7 nmol, which was 13.5% (mol/mol) of total analyzed lipids (Table 1), and corresponded to 45% of the cholesterol content of control cells (47.5 ± 5.4 nmol) (Fig. 7*A*; Table 1). Results from the Amplex® Red assay showed that MβCD-treated cells contained about 36% cholesterol of control cells.

In rafts, glycerophospholipids accounted for 49%, with PE representing 21% of the total analyzed rafts lipids. Cholesterol was the most abundant raft lipid representing 37% of analyzed raft lipids, whereas SM and GSLs accounted for 7% each (Fig. 7*B* and *D*). Analysis of the distribution of individual lipids in the gradients showed that 70% of GSLs, 56% of SM, and 47% of cholesterol were in the

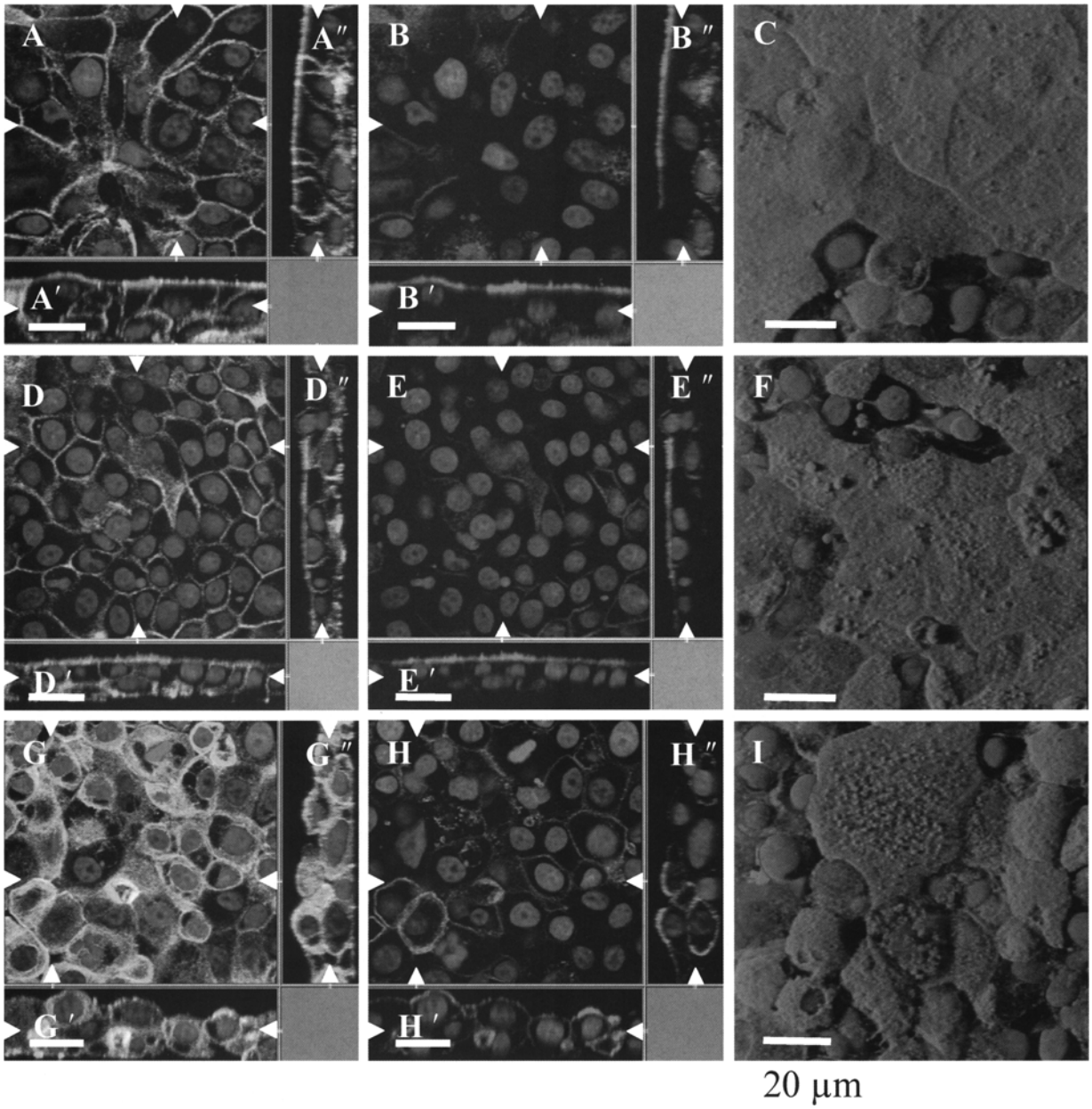

FIG. 1. Effect of methyl-β-cyclodextrin (MβCD) on the localization and distribution of P-glycoprotein (P-gp) in MDR1-MDCK cells. Cells were stained for P-gp (red), actin (green), and nuclei (blue) and studied by confocal laser scanning microscopy. *A–H* are xy-projections, (′), xz-projections, and (″), yz-projections. *Arrows* indicate the section levels. In *B*, *E*, and *H*, only P-gp and nuclei are shown for clarity, whereas *C*, *F*, and *I* are shadow projections. Most of P-gp was located in the apical membrane of both the control cells (*A–C*) and the cells treated with 30 m*M* MβCD (*D–F*). Treatment of cells with 100 m*M* MβCD resulted in an apparent decrease of P-gp (*G–I*) at the apical membrane and the residue labeling was punctuated. Figure is published in color online at http://inva.allenpress.com/invaonline/?request=index.html.

raft fractions (Fig. 7*B* and *C*). There was a significant decrease in the amount of cholesterol in the raft fractions of cells treated with 100 m*M* MβCD (Fig. 7*B*), and the residual cholesterol was 4.1 ± 1.6 nmol, which corresponded to 15% (mol/mol) of the cholesterol in raft fractions of control cells (27.6 ± 5.6 nmol). Instead of cholesterol, PE was the most abundant raft lipid constituting 24% of the raft lipids (Table 1). Cholesterol was also significantly decreased in the nonraft fractions after MβCD treatment (Fig. 7*C*).

The amount of GSLs in the cell lysates of PDMP-treated cells decreased significantly from 14.6 ± 2.8 in the control cells to 4.1 ± 1.6 nmol (Fig. 7*A*). The molar percentages of GSLs in the rafts and in nonraft fractions were in the same range as for the control cells (Fig. 7*B* and *C*).

The supernatant of control cells contained 2.7 ± 0.3 nmol cholesterol/mg protein and 0.2 ± 0.1 nmol GSLs/mg protein. The lipid–protein ratio increased significantly in the supernatant of cells treated with 100 m*M* MβCD to 7.2 ± 2.2 nmol/mg protein and 3.7 ± 2.7 nmol/mg protein, respectively.

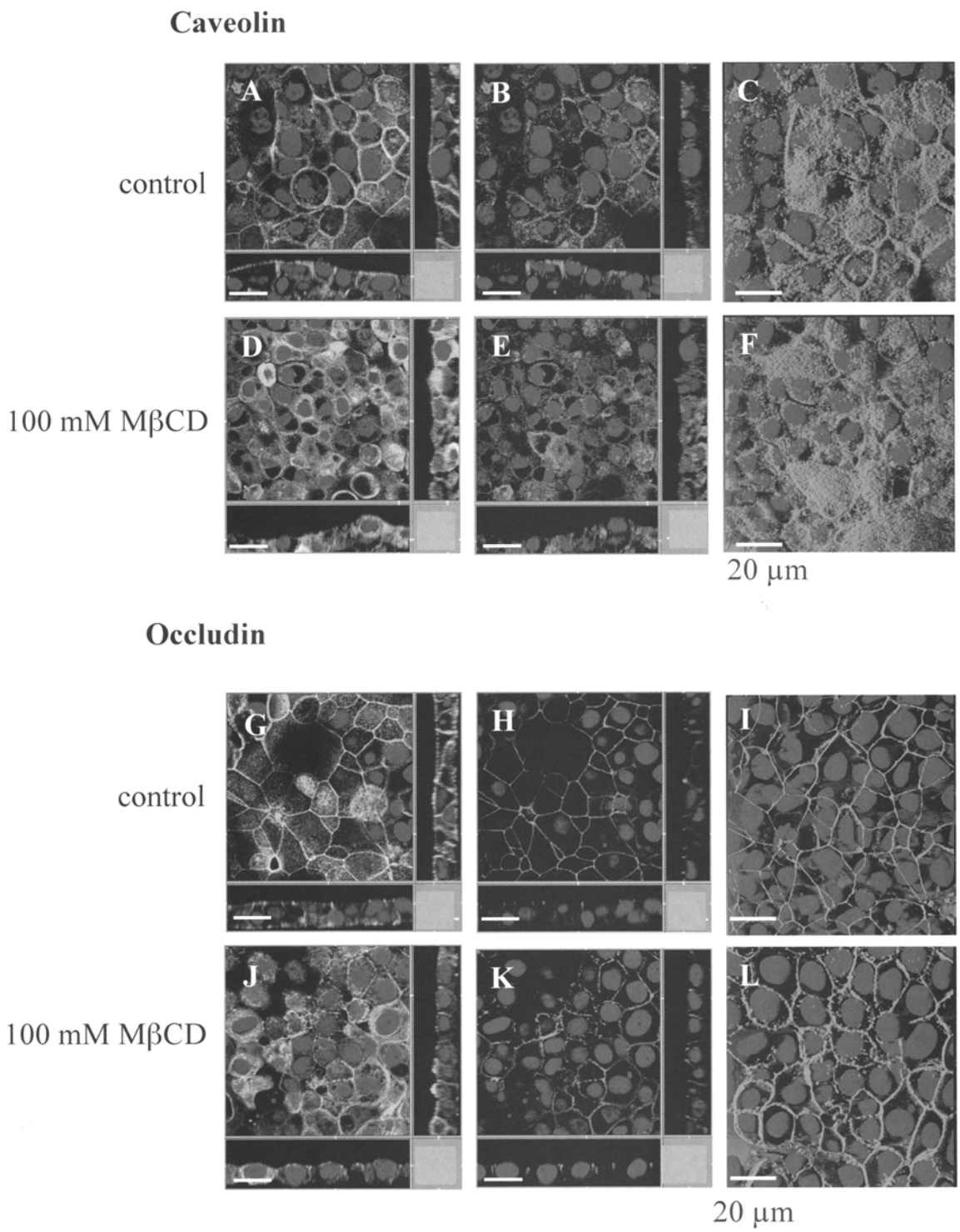

FIG. 2. Distribution of caveolin and occludin in MDR1-MDCK cells after methyl-β-cyclodextrin (MβCD) treatment. Immunolabeling of caveolin (*A–F*, red), occludin (*G–L*, red), actin (green), and nuclei (blue). Sections and shadow projections are as indicated in Fig. 1. There was no significant difference in the distribution of caveolin between control (*A–C*) and in cells treated with 100 m*M* MβCD (*D–E*). Occludin was still found in the cell borders of 100 m*M* MβCD-treated cells (*G–I*); however, tight junctions appeared loosened, and some intracellular staining was detected. Figure is published in color online at http://inva.allenpress.com/invaonline/?request=index.html.

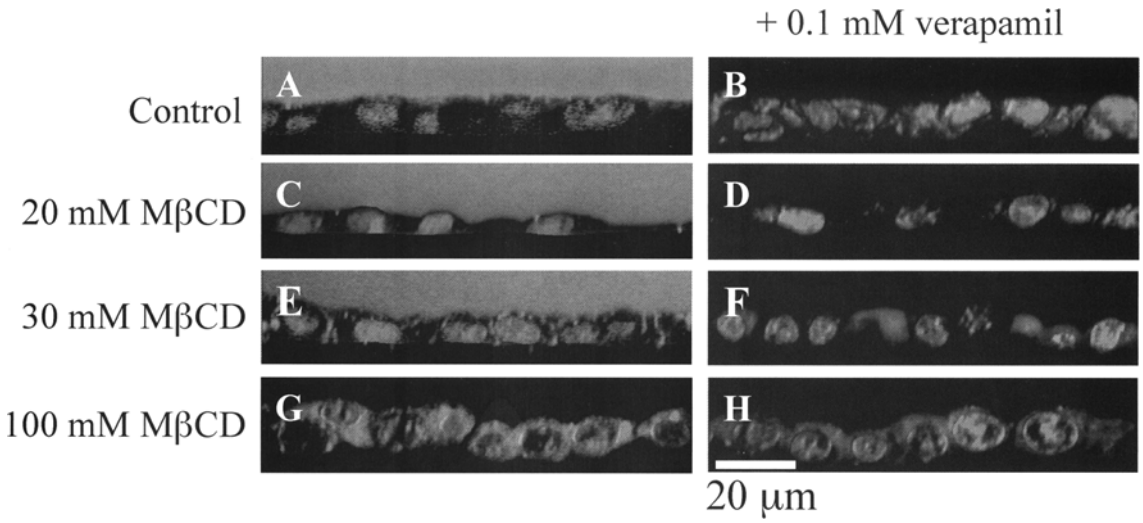

FIG. 3. Inhibition of efflux of rhodamine123 (rho123) from methyl-β-cyclodextrin (MβCD)–treated MDR1-MDCK cells. The efflux of rho123 from control and MβCD-treated cells was observed by confocal laser scanning microscopy. Rho123 (red) was effluxed to the extracellular space of control (*A*) and of 20 m*M* MβCD-treated cells (*C*). Some rho123 was retained in cells treated with 30 m*M* MβCD (*E*). Treatment with 100 m*M* MβCD resulted in a complete inhibition of rho123 efflux (*G*) to a similar extent as in cells treated with verapamil (*B*, *D*, *F*, and *H*). Nuclei (blue) are stained with Hoechst 33342. Figure is published in color online at http://inva.allenpress.com/invaonline/?request=index.html.

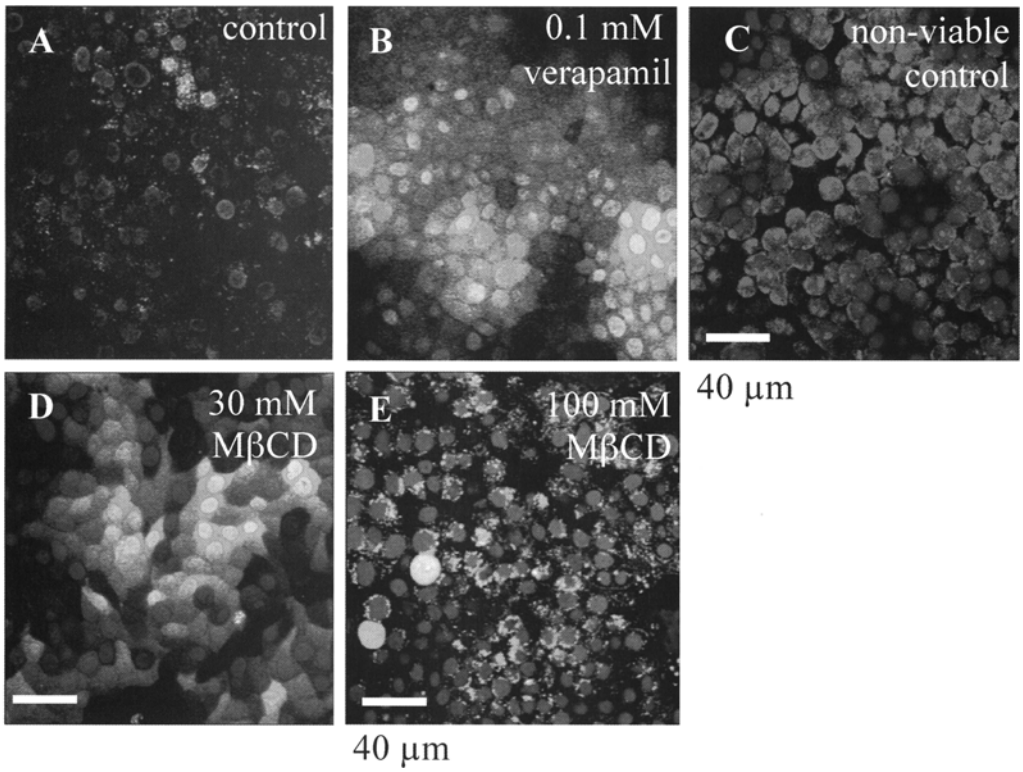

FIG. 4. Viability of methyl-β-cyclodextrin (MβCD)–treated MDR1-MDCK cells. The viability of control and MβCD-treated cells was tested with calcein AM and ethidium homodimer (Live/Dead Kit reagents). Treatment of cells with verapamil (*B*) inhibited the efflux of calcein AM and hence stronger green calcein staining than in the untreated control cells (*A*). No calcein was detected in nonviable cells (*C*), and ethidium homodimer permeated the cells resulting in red staining of the nuclei. Cells treated with 30 and 100 m*M* MβCD (*D* and *E*) were viable, and calcein AM was cleaved to green calcein. Nuclei (blue) are stained with Hoechst 33342. Figure is published in color online at http://inva.allenpress.com/invaonline/?request=index.html.

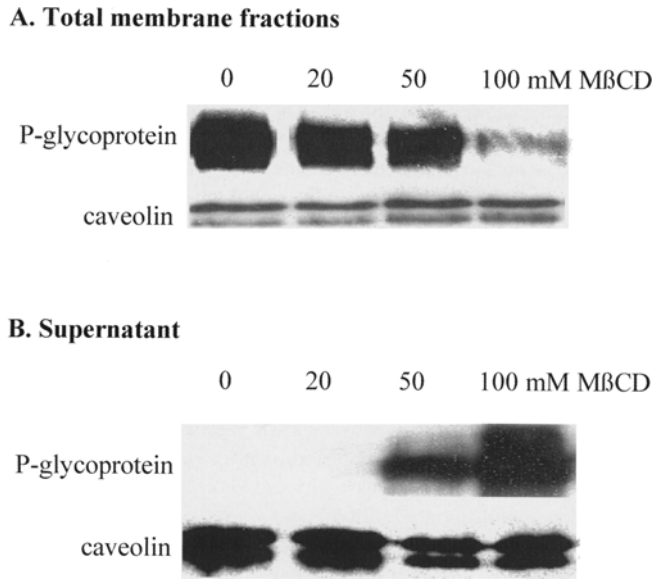

FIG. 5. Release of P-glycoprotein (P-gp) from cellular membranes of MDR1-MDCK cells. The P-gp and caveolin contents in total membranes treated with methyl-β-cyclodextrin (MβCD) (*A*) and in cell-free supernatants of cells treated with MβCD (*B*) were analyzed by immunoblotting. Treatment of total membrane with 100 m*M* MβCD resulted in a significant decrease of P-gp (*A*). A substantial amount of P-gp was released into the cell-free supernatant of cells treated with increased concentrations of MβCD, especially after treatment with 100 m*M* MβCD (*B*). The amount of caveolin in total membranes and in the supernatant remained unchanged despite the MβCD treatments (*A* and *B*).

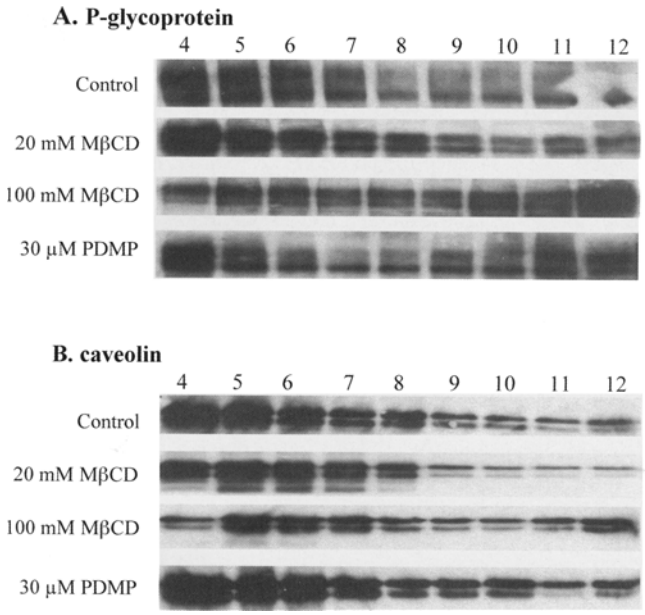

FIG. 6. Shift of P-glycoprotein (P-gp) from raft to nonraft fractions after methyl-β-cyclodextrin (MβCD) and 1-phenyl-2-decanoylamino-3-morpholino-1-propanolol (PDMP) treatment of MDR1-MDCK cells. The P-gp and caveolin contents in rafts (4–7) and nonrafts (8–12) fractions of cells treated with MβCD or PDMP were analyzed by immunoblotting. Treatment of cells with 100 m*M* MβCD and 30 μ*M* PDMP resulted in most of P-gp being shifted from the raft fractions to higher density fractions. The shift was only slight in cells treated with 20 m*M* MβCD for 30 min. Caveolin was not affected significantly by these treatments.

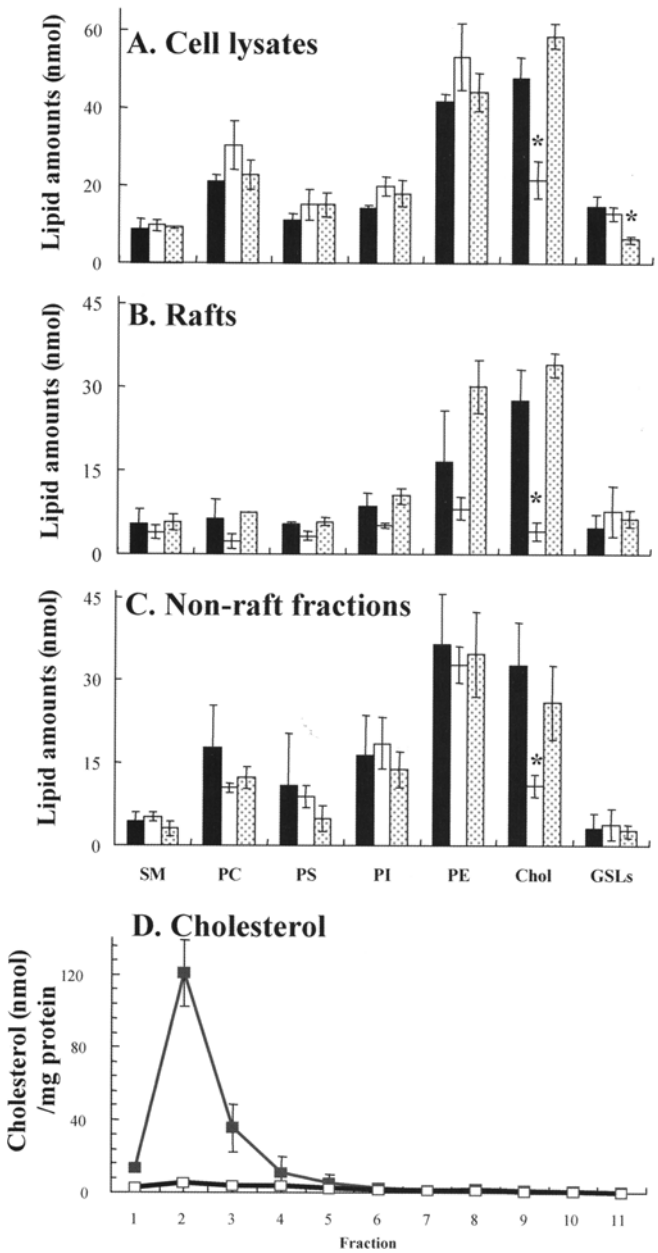

FIG. 7. Reduction of cholesterol and GSLs in methyl-β-cyclodextrin (MβCD)–and 1-phenyl-2-decanoylamino-3-morpholino-1-propanolol (PDMP)–treated MDR1-MDCK cells. Lipid composition of control cells (*black bars*) and cells treated with 100 m*M* MβCD (*unshaded bars*) or 30 μ*M* PDMP (*dotted bars*) were analyzed in the cell lysate (*A*), raft (*B*), and nonraft fractions (*C*), and the distribution of cholesterol (nmol/mg protein) in the sodium bromide gradient of control (■) and 100 m*M* MβCD-treated cells (□) were determined (*D*). Treatment of cells with MβCD resulted in a significant decrease of cholesterol, especially in the raft fractions. The amount of GSLs were decreased significantly in the cell lysates after treatment of cells with 30 μ*M* PDMP. Data represent the mean values ± S.D. of at least three independent experiments. Statistical significance compared with untreated cells is shown as (*) with $P < 0.05$. Abbreviations: SM, sphingomyelin; PC, phosphatidylcholine; PS, phosphatidylserine; PI, phosphatidylinositol; PE, phosphatidylethanolamine; Chol, cholesterol; GSL, glycosphingolipids.

TABLE 1

LIPID AND PROTEIN AMOUNTS IN CELL LYSATES, RAFT, AND NONRAFT FRACTIONS[a]

	Total lipids (nmol)	Total protein (mg)
Control		
Cell lysate	168.5 ± 12.2	72.3 ± 2.3
Rafts	75.0 ± 9.3	1.2 ± 0.5
Nonrafts	121.5 ± 8.9	18.1 ± 3.6
100 mM MβCD		
Cell lysate	161.7 ± 20.0	62.9 ± 4.5
Rafts	34.7 ± 8.5	1.1 ± 0.6
Nonrafts	90.6 ± 7.5	11.1 ± 3.2
30 μM PDMP		
Cell lysate	173.2 ± 13.7	73.3 ± 2.3
Rafts	100.2 ± 7.3	2.4 ± 0.8
Nonrafts	97.3 ± 9.1	20.3 ± 1.5

[a] Lipid and protein amounts in cell lysates, raft, and nonraft fractions of methyl-β-cyclodextrin (MβCD)– and PDMP-treated cells were analyzed, and data represent the mean amounts ± S.D. of ≥3 independent experiments. Treatment of cells with 100 m*M* MβCD resulted in decrease in amount of lipids especially in the raft fractions where the decrease was significant.

Discussion

The MDR1-MDCK cells expressing high amounts of P-gp on the apical plasma membrane represented an ideal system to elucidate the mechanisms of action of the protein after modulation of membrane lipid composition. Treatment of MDR1-MDCK cells with 100 m*M* MβCD reduced the amount of cholesterol in the total cell lysate, and the reduction was most significant in the raft fractions. This was accompanied by an apparent thinning out of the P-gp at the apical cell surface. Under these circumstances, efflux of rho123 was abolished, although the MβCD-treated cells remained viable. A recent study showed that P-gp interferes with the MTT assay (Vellonen et al., 2004); however, the cleavage of calcein AM and the exclusion of ethidium homodimer from the nuclei of cells treated with MβCD confirmed their viability. Our study indicates that the residual P-gp in MβCD-treated cells was not effective for the efflux of rho123. This was consistent with previous studies, which showed that depletion of cholesterol impaired P-gp–mediated drug transport in different cell lines (Luker et al., 2000; Yunomae et al., 2003; Arima et al., 2004). Our lipid and immunoblot analyses of the supernatant of MβCD-treated cells showed that cholesterol depletion was accompanied by release of large amounts of P-gp together with significant amounts of GSLs from the cell surface. The release or shedding of membrane components, which includes transmembrane proteins such as P-gp, CD30 glycoprotein, and interleukin-6 receptor, after cholesterol depletion, is a phenomenon that was also reported in previous studies (Xie and Low, 1995; Ilangumaran and Hoessli, 1998; Matthews et al., 2003; Yunomae et al., 2003; Arima et al., 2004; von Tresckow et al., 2004). In contrast to P-gp, caveolin was present in all the supernatants independent of MβCD treatment. When total membranes were treated with MβCD, P-gp was also released, whereas caveolin was not.

The raft-associated proteins, influenza virus hemagglutinin and placental alkaline phosphatase, were reported to shift from the raft to the nonraft fractions after MβCD treatment of cells (Scheiffele et al., 1997; Ilangumaran and Hoessli, 1998). In these studies, the effect was tentatively related to the disorganization and loss of integrity of rafts brought about in the membrane by the removal of cholesterol.

Our study showed that the removal of cholesterol with MβCD resulted in modulation of the lipid composition of the rafts. Cholesterol was no longer the most abundant lipid. This was accompanied by a shift of P-gp from the raft to the nonraft fractions. Caveolin localization in the rafts remained unchanged, consistent with results from previous studies (Scheiffele et al., 1997; Luker et al., 2000; Yunomae et al., 2003; Arima et al., 2004). This indicated a clear difference in the susceptibility of P-gp and caveolin to depletion of cholesterol. A heterogeneity in the lipid raft components in terms of their dependence on or interaction with cholesterol has been shown (Pike, 2003b). It can, thus, be hypothesized that the difference in susceptibility between P-gp and caveolin results from low MβCD accessibility of cholesterol within caveolae and a relatively high affinity between caveolin and cholesterol (Foster et al., 2003; Magee and Parmryd, 2003).

Investigations in our laboratory have shown that P-gp in rafts prepared from MDR1-MDCK cells have a distinct, substrate concentration-dependent ATPase activity (Bucher et al., 2005). No activity was found in rafts prepared from MβCD-treated cells. It remains to be demonstrated whether this loss of activity is because of the reduced amount of P-gp or cholesterol (or both) in the raft fractions, since the basal ATPase activity of P-gp reconstituted in proteoliposomes has been shown to increase on incorporation of cholesterol into the membrane (Rothnie et al., 2001; Modok et al., 2004). Further studies will confirm whether the loss of P-gp efflux activity after depletion of cholesterol is also because of the change of the lipid composition in the vicinity of P-gp.

There was a decrease of GSLs in the total cell lysate of MDR1-MDCK cells treated with PDMP, which was consistent with results from previous studies with 3LL carcinoma and Jurkat cells (Inokuchi et al., 2000; Nagafuku et al., 2003). Our study shows for the first time that in PDMP-treated cells, P-gp was shifted to the nonraft fractions. Similar results have been reported for the Src kinase, which is raft associated in control 3LL carcinoma cells but shifted to the nonraft fractions after treatment with PDMP (Inokuchi et al., 2000). Plo et al. (2002) showed that PDMP treatment also inhibits the efflux of rho123 by P-gp. In a recent study, Norris-Cervetto et al. (2004) came to the conclusion that chemosensitization of cells expressing P-gp could not be attributed to the inhibition of glucosylceramide synthase alone. The shift of P-gp from the raft fractions shown in our study could be an explanation for the loss of efflux activity of P-gp after PDMP treatment. Caveolin localization in the rafts was not affected by the PDMP treatment, which is in line with previous observations (Naslavsky et al., 1999).

To summarize, our study clearly showed that treatment of cells with MβCD and PDMP resulted in compound-specific modulations of the lipid composition of the cells, and both led to a shift of P-gp from raft to nonraft fractions. Removal of cholesterol resulted in the release of P-gp and GSLs from the membranes of intact cells and from total membranes. These modulations of the lipid composition resulted in loss of P-gp efflux activity in viable cells.

References

Arima, H.; Yunomae, K.; Morikawa, T.; Hirayama, F.; Uekama, K. Contribution of cholesterol and phospholipids to inhibitory effect of dimethyl-beta-cyclodextrin on efflux function of P-glycoprotein and multidrug resistance-associated protein 2 in vinblastine-resistant Caco-2 cell monolayers. Pharm. Res. 21:625–634; 2004.

Bradford, M. M. A rapid and sensitive method for the quantitation of microgram quantities of protein utilizing the principle of protein-dye binding. Anal. Biochem. 72:248–254; 1976.

Braun, A.; Hammerle, S.; Suda, K.; Rothen-Rutishauser, B.; Gunthert, M.; Kramer, S. D.; Wunderli-Allenspach, H. Cell cultures as tools in biopharmacy. Eur. J. Pharm. Sci. 11(Suppl. 2):S51–S60; 2000.

Brown, D. A.; Rose, J. K. Sorting of GPI-anchored proteins to glycolipid-enriched membrane subdomains during transport to the apical cell surface. Cell 68:533–544; 1992.

Bucher, K.; Besse, C. A.; Kamau, S. W.; Wunderli-Allenspach, H.; Krämer, S. D. Isolated rafts from adriamycin-resistant P388 cells contain functional ATPases and provide an easy test system for p-glycoprotein-related activities. Pharm. Res. 22:449–457; 2005.

Demeule, M.; Jodoin, J.; Gingras, D.; Beliveau, R. P-glycoprotein is localized in caveolae in resistant cells and in brain capillaries. FEBS Lett. 466:219–224; 2000.

di Bartolomeo, S.; Spinedi, A. Differential chemosensitizing effect of two glucosylceramide synthase inhibitors in hepatoma cells. Biochem. Biophys. Res. Commun. 288:269–274; 2001.

Eytan, G. D.; Kuchel, P. W. Mechanism of action of P-glycoprotein in relation to passive membrane permeation. Int. Rev. Cytol. 190:175–250; 1999.

Fontaine, M.; Elmquist, W. F.; Miller, D. W. Use of rhodamine 123 to examine the functional activity of P-glycoprotein in primary cultured brain microvessel endothelial cell monolayers. Life Sci. 59:1521–1531; 1996.

Foster, L. J.; De Hoog, C. L.; Mann, M. Unbiased quantitative proteomics of lipid rafts reveals high specificity for signaling factors. Proc. Natl. Acad. Sci. USA 100:5813–5818; 2003.

Hammerle, S. P.; Rothen-Rutishauser, B.; Kramer, S. D.; Gunthert, M.; Wunderli-Allenspach, H. P-Glycoprotein in cell cultures: a combined approach to study expression, localisation, and functionality in the confocal microscope. Eur. J. Pharm. Sci. 12:69–77; 2000.

Hooper, N. M. Detergent-insoluble glycosphingolipid/cholesterol-rich membrane domains, lipid rafts and caveolae (review). Mol. Membr. Biol. 16:145–156; 1999.

Ilangumaran, S.; Hoessli, D. C. Effects of cholesterol depletion by cyclodextrin on the sphingolipid microdomains of the plasma membrane. Biochem. J. 335(Pt. 2):433–440; 1998.

Inokuchi, J. I.; Uemura, S.; Kabayama, K.; Igarashi, Y. Glycosphingolipid deficiency affects functional microdomain formation in Lewis lung carcinoma cells. Glycoconj. J. 17:239–245; 2000.

Kohler, S.; Stein, W. D. Optimizing chemotherapy by measuring reversal of P-glycoprotein activity in plasma membrane vesicles. Biotechnol. Bioeng. 81:507–517; 2003.

Kramer, S. D.; Hurley, J. A.; Abbott, N. J.; Begley, D. J. Lipids in blood-brain barrier models in vitro I: thin-layer chromatography and high-performance liquid chromatography for the analysis of lipid classes and long-chain polyunsaturated fatty acids. In Vitro Cell. Dev. Biol. 38A:557–565; 2002.

Laemmli, U. K. Cleavage of structural proteins during the assembly of the head of bacteriophage T4. Nature 227:680–685; 1970.

Lavie, Y.; Cao, H.; Volner, A.; Lucci, A.; Han, T. Y.; Geffen, V.; Giuliano, A. E.; Cabot, M. C. Agents that reverse multidrug resistance, tamoxifen, verapamil, and cyclosporin A, block glycosphingolipid metabolism by inhibiting ceramide glycosylation in human cancer cells. J. Biol. Chem. 272:1682–1687; 1997.

Lavie, Y.; Fiucci, G.; Czarny, M.; Liscovitch, M. Changes in membrane microdomains and caveolae constituents in multidrug-resistant cancer cells. Lipids 34(Suppl.):S57–S63; 1999.

Lavie, Y.; Fiucci, G.; Liscovitch, M. Up-regulation of caveolae and caveolar constituents in multidrug-resistant cancer cells. J. Biol. Chem. 273:32380–32383; 1998.

Loor, F.; Tiberghien, F.; Wenandy, T.; Didier, A.; Traber, R. Cyclosporins: structure-activity relationships for the inhibition of the human MDR1 P-glycoprotein ABC transporter. J. Med. Chem. 45:4598–4612; 2002.

Lucci, A.; Han, T. Y.; Liu, Y. Y.; Giuliano, A. E.; Cabot, M. C. Modification of ceramide metabolism increases cancer cell sensitivity to cytotoxics. Int. J. Oncol. 15:541–546; 1999.

Luker, G. D.; Pica, C. M.; Kumar, A. S.; Covey, D. F.; Piwnica-Worms, D. Effects of cholesterol and enantiomeric cholesterol on P-glycoprotein localization and function in low-density membrane domains. Biochemistry 39:7651–7661; 2000.

Magee, A. I.; Parmryd, I. Detergent-resistant membranes and the protein composition of lipid rafts. Genome Biol. 4:234; 2003.

Matthews, V.; Schuster, B.; Schutze, S., et al. Cellular cholesterol depletion triggers shedding of the human interleukin-6 receptor by ADAM10 and ADAM17 (TACE). J. Biol. Chem. 278:38829–38839; 2003.

Modok, S.; Heyward, C.; Callaghan, R. P-glycoprotein retains function when reconstituted into a sphingolipid- and cholesterol-rich environment. J. Lipid Res. 45:1910–1918; 2004.

Mosmann, T. Rapid colorimetric assay for cellular growth and survival: application to proliferation and cytotoxicity assays. J. Immunol. Methods 65:55–63; 1983.

Nagafuku, M.; Kabayama, K.; Oka, D., et al. Reduction of glycosphingolipid levels in lipid rafts affects the expression state and function of glycosylphosphatidylinositol-anchored proteins but does not impair signal transduction via the T cell receptor. J. Biol. Chem. 278:51920–51927; 2003.

Naslavsky, N.; Shmeeda, H.; Friedlander, G.; Yanai, A.; Futerman, A. H.; Barenholz, Y.; Taraboulos, A. Sphingolipid depletion increases formation of the scrapie prion protein in neuroblastoma cells infected with prions. J. Biol. Chem. 274:20763–20771; 1999.

Neethling, F. A.; Koscec, M.; Oriol, R.; Cooper, D. K.; Koren, E. A reliable, rapid and inexpensive two-color fluorescence assay to monitor serum cytotoxicity in xenotransplantation. J. Immunol. Methods 222:31–44; 1999.

Norris-Cervetto, E.; Callaghan, R.; Platt, F. M.; Dwek, R. A.; Butters, T. D. Inhibition of glucosylceramide synthase does not reverse drug resistance in cancer cells. J. Biol. Chem. 279:40412–40418; 2004.

Pastan, I.; Gottesman, M. M.; Ueda, K.; Lovelace, E.; Rutherford, A. V.; Willingham, M. C. A retrovirus carrying an MDR1 cDNA confers multidrug resistance and polarized expression of P-glycoprotein in MDCK cells. Proc. Natl. Acad. Sci. USA 85:4486–4490; 1988.

Pike, L. J. Lipid rafts: bringing order to chaos. J. Lipid Res. 44:655–667; 2003a.

Pike, L. J. Lipid rafts: heterogeneity on the high seas. Biochem. J. 378:281–292; 2003b.

Plo, I.; Lehne, G.; Beckstrom, K. J.; Maestre, N.; Bettaieb, A.; Laurent, G.; Lautier, D. Influence of ceramide metabolism on P-glycoprotein function in immature acute myeloid leukemia KG1a cells. Mol. Pharmacol. 62:304–312; 2002.

Roepe, P. D. The P-glycoprotein efflux pump: how does it transport drugs? J. Membr. Biol. 166:71–73; 1998.

Rothen-Rutishauser, B.; Kramer, S. D.; Braun, A.; Gunthert, M.; Wunderli-Allenspach, H. MDCK cell cultures as an epithelial in vitro model: cytoskeleton and tight junctions as indicators for the definition of age-related stages by confocal microscopy. Pharm. Res. 15:964–971; 1998.

Rothnie, A.; Theron, D.; Soceneantu, L., et al. The importance of cholesterol in maintenance of P-glycoprotein activity and its membrane perturbing influence. Eur. Biophys. J. 30:430–442; 2001.

Scheiffele, P.; Roth, M. G.; Simons, K. Interaction of influenza virus haemagglutinin with sphingolipid-cholesterol membrane domains via its transmembrane domain. EMBO J. 16:5501–5508; 1997.

Shand, J. H.; Noble, R. C. Quantification of lipid mass by a liquid scintillation counting procedure following charring on thin-layer plates. Anal. Biochem. 101:427–434; 1980.

Sharom, F. J. The P-glycoprotein efflux pump: how does it transport drugs? J. Membr. Biol. 160:161–175; 1997.

Sietsma, H.; Veldman, R. J.; Kolk, D.; Ausema, B.; Nijhof, W.; Kamps, W.; Vellenga, E.; Kok, J. W. 1-phenyl-2-decanoylamino-3-morpholino-1-propanol chemosensitizes neuroblastoma cells for taxol and vincristine. Clin. Cancer Res. 6:942–948; 2000.

Simons, K.; Ikonen, E. Functional rafts in cell membranes. Nature 387:569–572; 1997.

Simons, K.; van Meer, G. Lipid sorting in epithelial cells. Biochemistry 27:6197–6202; 1988.

Tang, F.; Horie, K.; Borchardt, R. T. Are MDCK cells transfected with the human MDR1 gene a good model of the human intestinal mucosa? Pharm. Res. 19:765–772; 2002.

Troost, J.; Albermann, N.; Emil Haefeli, W.; Weiss, J. Cholesterol modulates P-glycoprotein activity in human peripheral blood mononuclear cells. Biochem. Biophys. Res. Commun. 316:705–711; 2004.

van de Loosdrecht, A. A.; Beelen, R. H.; Ossenkoppele, G. J.; Broekhoven, M. G.; Langenhuijsen, M. M. A tetrazolium-based colorimetric MTT assay to quantitate human monocyte mediated cytotoxicity against leukemic cells from cell lines and patients with acute myeloid leukemia. J. Immunol. Methods 174:311–320; 1994.

Vellonen, K. S.; Honkakoski, P.; Urtti, A. Substrates and inhibitors of efflux proteins interfere with the MTT assay in cells and may lead to underestimation of drug toxicity. Eur. J. Pharm. Sci. 23:181–188; 2004.

von Treskow, B.; Kallen, K. J.; von Strandmann, E. P.; Borchmann, P.; Lange, H.; Engert, A.; Hansen, H. P. Depletion of cellular cholesterol and lipid rafts increases shedding of CD30. J. Immunol. 172:4324–4331; 2004.

Wagner, M. M.; Paul, D. C.; Shih, C.; Jordan, M. A.; Wilson, L.; Williams, D. C. In vitro pharmacology of cryptophycin 52 (LY355703) in human tumor cell lines. Cancer Chemother. Pharmacol. 43:115–125; 1999.

Xie, M.; Low, M. G. Streptolysin-O induces release of glycosylphosphatidylinositol-anchored alkaline phosphatase from ROS cells by vesiculation independently of phospholipase action. Biochem. J. 305(Pt. 2):529–537; 1995.

Yunomae, K.; Arima, H.; Hirayama, F.; Uekama, K. Involvement of cholesterol in the inhibitory effect of dimethyl-beta-cyclodextrin on P-glycoprotein and MRP2 function in Caco-2 cells. FEBS Lett. 536:225–231; 2003.

Zhou, M.; Diwu, Z.; Panchuk-Voloshina, N.; Haugland, R. P. A stable nonfluorescent derivative of resorufin for the fluorometric determination of trace hydrogen peroxide: applications in detecting the activity of phagocyte NADPH oxidase and other oxidases. Anal. Biochem. 253:162–168; 1997.